Published as: *Cell*. 2010 November 24; 143(5): 774–788.

Mechanisms determining the morphology of the peripheral ER

Yoko Shibata[1,2], **Tom Shemesh**[3], **William A. Prinz**[4], **Alexander F. Palazzo**[1,5], **Michael M. Kozlov**[3,*], and **Tom A. Rapoport**[1,2,*]

[1] Howard Hughes Medical Institute, Harvard Medical School, 240 Longwood Avenue, Boston, MA 02115, USA

[2] Department of Cell Biology, Harvard Medical School, 240 Longwood Avenue, Boston, MA 02115, USA

[3] Department of Physiology and Pharmacology, Sackler Faculty of Medicine, Tel Aviv University, Ramat Aviv, 69978 Tel Aviv, Israel

[4] Laboratory of Cell Biochemistry and Biology, National Institute of Diabetes and Digestive and Kidney Disorders, National Institute of Health, Bethesda, MD 02892, USA

[5] Department of Biochemistry, University of Toronto, 1 King's College Circle, Toronto, ON M5S 1A8, Canada

Abstract

The endoplasmic reticulum (ER) consists of the nuclear envelope and a peripheral network of tubules and membrane sheets. The tubules are shaped by the curvature-stabilizing proteins reticulons and DP1/Yop1p, but how the sheets are formed is unclear. Here we identify several sheet-enriched membrane proteins in the mammalian ER, including proteins that translocate and modify newly synthesized polypeptides, as well as coiled-coil membrane proteins that are highly upregulated in cells with proliferated ER sheets, all of which are localized by membrane-bound polysomes. These results indicate that sheets and tubules correspond to rough and smooth ER, respectively. One of the coiled-coil proteins, Climp63, serves as a "luminal ER spacer" and forms sheets when overexpressed. More universally, however, sheet-formation appears to involve the reticulons and DP1/Yop1p, which localize to sheet edges and whose abundance determines the ratio of sheets to tubules. These proteins may generate sheets by stabilizing the high curvature of edges.

Introduction

How the characteristic shape of a membrane-bound organelle is generated is a fundamental question in cell biology. We have started to address this question for the endoplasmic reticulum (ER), an organelle that has a particularly intriguing morphology. It is a continuous membrane system that is comprised of the nuclear envelope as well as of a peripheral network of tubules and sheets (Baumann and Walz, 2001; Shibata et al., 2009; Voeltz et al., 2002). Both the tubules and sheets are dynamic, i.e. they are continuously forming and collapsing. Previous work has identified proteins that are responsible for shaping the tubular ER network (Hu et al., 2008; Hu et al., 2009; Shibata et al., 2008; Voeltz et al., 2006), but

*Correspondence: tom_rapoport@hms.harvard.edu (T.A.R.); phone: 617-432-0676; 617-432-1612 or michk@post.tau.ac.il (M.M.K.).

essentially nothing is known about how ER sheets are generated. In addition, it is unknown whether proteins specifically segregate into ER sheets and whether there is a functional significance to the existence of different ER morphologies.

ER tubules are characterized by high membrane curvature in cross-section and shaped by two families of curvature-stabilizing proteins, the reticulons and DP1/Yop1p (Voeltz et al., 2006). Members of both families are ubiquitously expressed in all eukaryotic cells. These proteins localize to the ER tubules and their depletion leads to the loss of tubules. Conversely, the overexpression of certain isoforms results in long, unbranched tubules. Purified members of the two families deform reconstituted proteoliposomes into tubules (Hu et al., 2008). Together, these results indicate that the reticulons and DP1/Yop1p are both necessary and sufficient for ER tubule formation. These two protein families do not share sequence homology, but both have a conserved domain containing two long hydrophobic segments that sit in the membrane as hairpins (Voeltz et al., 2006). These hairpins may stabilize the high curvature of tubules in cross-section by forming a wedge in the lipid bilayer. In addition, oligomerization of these proteins may generate arc-like scaffolds around the tubules (Shibata et al., 2008).

The peripheral ER sheets vary in size, but always consist of two closely apposed membranes whose distance is approximately the same as the diameter of the tubules (~50 nm in mammals and ~30 nm in yeast; (Bernales et al., 2006). Consequently, the edges of sheets have a similarly high curvature as the cross-section of tubules. In “professional” secretory cells, such as plasma B cells or pancreatic cells, the ER sheets extend throughout the entire cell and are studded with membrane-bound ribosomes. They are stacked tightly with regular distances between the membranes on both the cytoplasmic and luminal sides (Fawcett, 1981). By contrast, cells that do not secrete many proteins contain mostly tubular ER. These observations have led to the idea that ER sheets correspond to rough ER (Shibata et al., 2006), the region of the ER that contains membrane-bound ribosomes, i.e. ribosomes associated with the translocons, the sites of translocation and modification of newly synthesized secretory and membrane proteins. On the other hand, ER tubules would correspond to smooth ER (Shibata et al., 2006), the ER region devoid of ribosomes, which may be specialized in lipid metabolism or Ca^{2+} signaling. While these ideas are attractive, the tubular ER clearly contains membrane-bound ribosomes, and a segregation of rough ER proteins into sheets has not yet been demonstrated.

Several mechanisms of ER sheet formation have been considered. One possibility is that integral membrane proteins would form bridges across the luminal space of the ER (Senda and Yoshinaga-Hirabayashi, 1998; Shibata et al., 2009). A second possibility is that proteins form flat cytoplasmic or luminal scaffolds, as suggested for the formation of flat Golgi cisternae (Short et al., 2005). It has also been proposed that the membrane association of ribosomes could directly be responsible for the generation of ER sheets (Puhka et al., 2007). Finally, given that the reticulons and DP1/Yop1p generate high curvature membranes, one might imagine that they generate sheets by stabilizing the sheet edges, bringing the apposing membranes in close proximity (Shibata et al., 2009).

Here we show that rough ER proteins partition into ER sheets. This includes both proteins involved in translocation and modification of newly synthesized polypeptides, as well as coiled-coil membrane proteins that are highly upregulated in cells containing proliferated ER sheets. Membrane-bound polysomes are required for the segregation of these rough ER proteins into sheets, and one of the coiled-coil proteins, Climp63, serves as a luminal ER spacer. However, neither the polysomes nor the coiled-coil proteins are essential for sheet formation *per se*. Instead, a major mechanism of sheet formation appears to involve the reticulons and DP1/Yop1p proteins, which can stabilize the high membrane curvature at

sheet edges. Our results suggest that in many cells their abundance is the major determinant of ER morphology.

Results

Segregation of proteins into ER sheets

The different morphologies of the ER imply that, despite the continuity of the membrane system, some proteins are likely enriched in certain domains. So far, the only proteins known with a specific localization are the tubule-preferring reticulons, DP1/Yop1p, and atlastins/Sey1p (Hu et al., 2009; Shibata et al., 2008; Voeltz et al., 2006). These proteins localize to tubules even when highly overexpressed. By contrast, other overexpressed ER proteins distribute indiscriminately throughout the entire ER, making it impossible to draw conclusions about their endogenous localizations. We therefore first tested whether several endogenous ER proteins segregate into different ER domains using immunofluorescence and confocal microscopy in BSC1 cells. As expected, the luminal ER protein calreticulin, which is involved in the folding of glycoproteins, was found in peripheral ER sheets, which are mostly located close to the nucleus, as well as in the tubular ER network and the nuclear envelope (Figure 1A). Calreticulin perfectly co-localized with GFP-tagged Sec61β, stably overexpressed in the same cell. Endogenous Sec61β is part of the Sec61 complex, the component forming the protein-conducting channel in the ER, but due to its tagging with GFP and overexpression, GFP-Sec61β is not associated with the translocon and distributes throughout the ER (Shibata et al., 2008). Antibodies recognizing the luminal chaperones BiP and Grp94 (anti-KDEL) also stained the entire ER (Figure 1C, middle panel). The integral membrane proteins calnexin and Bap31 showed a similar ubiquitous localization as overexpressed GFP-Sec61β (Figures 1B and S1). These results suggest that many luminal and membrane ER proteins do not localize to a specific ER domain, consistent with the continuity of the membrane system.

Next we tested the endogenous localization of components of the translocon. In contrast to overexpressed GFP-Sec61β, endogenous Sec61β was found concentrated in ER sheets when compared to the localization of the luminal ER proteins BiP and GRP94, although some weak staining of the tubular network and non-specific staining of the cytoplasm were also seen (Figure 1C). Because endogenous Sec61β is contained in the Sec61 complex, these data suggest that translocons are enriched in ER sheets. This is supported by the localization of endogenous TRAPα, a component tightly associated with the ribosome-bound Sec61 complex (Menetret et al., 2008); TRAPα was strongly enriched in the peripheral ER sheets (Figure 1D). Finally, Dad1, a component of the translocon-associated oligosaccharyl transferase complex that glycosylates nascent secretory and membrane proteins, also showed a similar localization; GFP-tagged Dad1 that was stably expressed in Dad1-deficient cells at a level just sufficient to sustain viability (Nikonov et al., 2002), showed a clear preference for ER sheets, in contrast to calreticulin in the same cell (Figure 1E). Together, these data indicate that translocon components are enriched in ER sheets.

To identify additional sheet-segregating proteins that could potentially even be required for sheet formation, we reasoned that such proteins would be abundant in highly secretory cells that contain proliferated ER sheets. We therefore identified by mass spectrometry the most abundant, integral ER membrane proteins in dog pancreatic rough microsomes. The 25 most abundant proteins include translocon components, such as subunits of the oligosaccharyl transferase complex, signal peptidase, SRP receptor, components of the TRAP complex, and the Sec61 complex (Table S1). Interestingly, the list also includes p180 and Climp63. Kinectin, which is sequence-related to p180, is somewhat less abundant. All of these proteins have a single transmembrane segment and an extended coiled-coil domain, which is located on the luminal side of the ER membrane in the case of Climp63, and on the

cytoplasmic side in the case of p180 and kinectin (Figure S2A). The molecular function of these coiled-coil proteins is not well understood. Climp63 has been implicated in the interaction of ER membranes with microtubules (Klopfenstein et al., 1998). P180 was originally proposed to be a ribosome receptor (Savitz and Meyer, 1990); it also interacts with microtubules (Ogawa-Goto et al., 2007) and is now thought to play a role in the differentiation of certain monocytic cells (Benyamini et al., 2009). Kinectin was initially identified as a receptor for the molecular motor kinesin (Toyoshima et al., 1992).

Another way to identify potential sheet-segregating proteins is to analyze components that are upregulated during the differentiation of immature B-cells to IgG-secreting plasma cells, which involves massive ER sheet proliferation. To identify mRNAs whose abundance is greatly increased, we used published microarray data (Luckey et al., 2006). The list of the 25 most upregulated mRNAs coding for ER membrane proteins (Table S2) includes components of the translocon, of the unfolded protein response, and of the ER protein degradation machinery. It also includes Climp63 and p180 (their mRNAs are upregulated by a factor of 19–26; kinectin mRNA was not analyzed). Together with the mass-spectrometry data, these results raise the possibility that the coiled-coil membrane proteins Climp63, p180, and kinectin localize to ER sheets. Because these proteins have no known function in protein translocation or modification, they are also candidates for being involved in sheet formation.

Next we tested whether the coiled-coil proteins are enriched in ER sheets, using immunofluorescence and confocal microscopy. At endogenous levels, all three proteins indeed segregated to ER sheets, whereas in the same cells, calreticulin distributed throughout the entire ER (Figure 2A–C). P180-GFP overexpressed at moderate levels was also enriched in ER sheets (Figure S2B). Thus, in addition to the translocon proteins, at least three other abundant integral membrane proteins are enriched in ER sheets. All three proteins were noticeably depleted from the nuclear envelope (Figure 2 and S2), as reported previously for Climp63 (Klopfenstein et al., 1998).

A role for polysomes in protein enrichment in ER sheets

Because translocon-associated proteins were found enriched in ER sheets and are generally associated with ribosomes, we tested whether the sheet-preferring proteins are localized by their association with membrane-bound translating ribosomes. We treated tissue culture cells with puromycin, a drug that releases nascent polypeptide chains from ribosomes and disassembles polysomes; the localization of endogenous sheet-preferring proteins was subsequently analyzed by immunofluorescence. TRAPα moved out of the sheets into the tubular network (Figure 3A). Quantification shows that in untreated cells TRAPα is enriched in sheets, as compared to the general ER marker GFP-Sec61β, but 15 min after puromycin addition, TRAPα was almost equally abundant in sheets and tubules (Figure 3E). The disassembly of the polysomes did not abolish the ER sheets, which in fact occupied a larger surface in many cells (Figure S3A). To rule out the possibility that inhibition of translation causes the redistribution of TRAPα, we performed control experiments with cycloheximide, a drug that inhibits the elongation of polypeptide chains but leaves polysomes intact. Cycloheximide inhibited protein synthesis as effectively as puromycin (Figure S4), but TRAPα stayed in ER sheets (Figure 3B, 3E). All the other tested ER-sheet preferring proteins behaved in the same way as TRAPα (Figure 3C–3E). On the other hand, the localization of calnexin and BAP31, membrane proteins that did not segregate into ER sheets, remained unchanged after treatment with either puromycin or cycloheximide, as was also the case for the luminal protein calreticulin (Figures 3E and S3B, C). Pactamycin, an inhibitor of translation initiation, which allows ribosomes to run-off the mRNAs, had a similar effect as puromycin on sheet-segregating proteins, i.e. they were no longer concentrated in sheets (Figure S3D). Again, the sheets did not disappear but rather occupied

a larger area of the cell (Figure S3E). These results indicate that polysomes concentrate sheet domains and localize certain membrane proteins to ER sheets, likely because these proteins have a direct or indirect affinity for membrane-bound polysomes.

Climp63 serves as a "luminal ER spacer"

To test for a possible role of the coiled-coil membrane proteins in ER morphology, we performed RNAi experiments. The depletion of Climp63, p180, and kinectin (Figure S5A) either individually or together did not abolish the existence of ER sheets (Figure 2D vs. 2E). Nevertheless, these proteins have an effect on ER morphology, as the sheets in depleted cells spread throughout the cytoplasm (Figure S5C–D), similarly to what is observed when cells are treated with puromycin or pactamycin (Figure S3). It thus seems that the coiled-coil membrane proteins are not required for sheet formation *per se*, but function in segregating sheet domains close to the cell nucleus.

Thin-section electron microscopy of COS7 cells confirmed that peripheral ER sheets persist after puromycin treatment or depletion of Climp63, p180, and kinectin (compare Figures 4B and C with 4A). No bulging of the two membrane sheets was observed, but interestingly, the luminal width was significantly reduced in triple knock-down cells (from 45–50 nm to 25–30 nm; Figure 4E). A similar effect was seen when Climp63 alone was depleted (Figure 4D), whereas single or double knock-down of p180 and kinectin had no obvious phenotype (Figure 4E, and data not shown). These results indicate that Climp63 serves to maintain the normal luminal width of peripheral ER sheets, likely by forming bridges through their luminal coiled-coil domains (Klopfenstein et al., 2001).. Consistent with a luminal spacer function, organisms that lack Climp63, including Drosophila S2 cells (Figure 4E), silkworm (Senda and Yoshinaga-Hirabayashi, 1998), and S. cerevisiae (Bernales et al., 2006), all appear to have narrower ER sheets than mammals. It should be noted that the distance between the inner and outer nuclear membranes was unaffected by Climp63-depletion and was the same in mammalian and insect cells (Figure 4E), consistent with the absence of this protein from the nuclear envelope.

Linking the formation of ER sheets and tubules

The overexpression of Climp63 led to a dramatic proliferation of ER sheets; we observed a good correlation between the expression level of a FLAG-tagged version of Climp63 in COS7 cells and the generation of sheets, an effect that is most strikingly seen in 3D reconstructions of the ER (Figures 5A–B; quantification in Figure 5C). In thin-section electron microscopy prominent membrane structures were seen that consisted of anastomosing sheets containing membrane-bound ribosomes (Figure 5D). The sheets had a constant luminal width of ~50 nm, and at the highest expression levels the luminal protein calreticulin was displaced from areas of Climp63 localization (Figure S6), consistent with Climp63 filling the luminal space. We also observed "organized smooth ER (OSER)" structures in which the membranes were tightly stacked and the internal membranes were devoid of ribosomes (Figure S7). Although these structures are likely caused by oligomerization of the cytoplasmic GFP tag (Snapp et al., 2003), they differ from normal OSERs by having a constant luminal spacing of ~50 nm.

Given that ER sheet proliferation was also observed when the curvature-stabilizing reticulons are depleted in mammalian cells by RNAi (Anderson and Hetzer, 2008), or when the reticulons and Yop1p are lacking in *S. cerevisiae* (Voeltz et al., 2006), we tested whether Climp63 and the reticulons have opposing effects on ER sheet formation. Indeed, when the reticulon Rtn4b was overexpressed in COS7 cells, peripheral ER sheets became diminished with increasing expression levels (Figures 5E–F; quantification in Figure 5G and H). Concomitant with the decrease in sheet structures, the normal tubular network was gradually

replaced with long, unbranched tubules (quantification in Figure 5I). When Climp63 and Rtn4a were both highly overexpressed, the normal ER morphology was almost restored (Figure 5J). Taken together, these results indicate that Climp63 and the curvature-promoting proteins undergo a "tug-of-war" that determines the amount of membrane partitioning into these domains.

Curvature-stabilizing proteins localize to sheet edges

Because the reticulons and DP1/Yop1p localize to tubules, one might expect that they are also found at sheets edges since these have a similarly high membrane curvature as tubules in cross-section. Indeed, in many cells the endogenous reticulons localized to the edges of sheets, as demonstrated by immunofluorescence using antibodies recognizing both Rtn4a and 4b (Figure 6A). Similar observations were made in plant cells (Sparkes et al., 2010). In Climp63 overexpressing cells with proliferated sheets, Rtn4a/b lined the edges of essentially all sheets in an even more striking manner (Figure 6B).

To test whether the curvature-stabilizing proteins generally localize to sheet edges, we tested the localization of a reticulon in *S. cerevisiae*. We expressed GFP-Rtn1p from the chromosome together with ssRFP-HDEL, a general, luminal ER marker. Indeed, peripheral ER sheets were generally lined by GFP-Rtn1p (Figure 6C). The edge localization of GFP-Rtn1p was even more obvious in cells where ER sheet proliferation was induced by deletion of the genes encoding the tubule-shaping protein Yop1p and the GTPase Sey1p (Figure 6D; (Hu et al., 2009). Similar results were obtained when ER sheets were induced by deletion of *OPI1* (Figure 6E; (Schuck et al., 2009). Thus, as in mammalian cells, the reticulons localize to the edges of peripheral ER sheets. These results indicate that the reticulons stabilize the high curvature of both tubules in cross-section and of sheet edges.

A role for curvature-stabilizing proteins in sheet formation

Given the localization of the curvature-generating proteins to sheet-edges, we considered the possibility that they can generate sheets by bringing the apposing membranes into close proximity. In this model, the ratio of sheets and tubules would be determined by the relative amounts of lipids and curvature-stabilizing proteins. Indeed, the sheet proliferation seen upon *OPI1* deletion in *S. cerevisiae* (Figure 6E) is likely caused by an increase in phospholipid synthesis; Opi1p normally inhibits the transcriptions factors Ino2p and Ino4p, which control many phospholipid synthesis enzymes (Ambroziak and Henry, 1994; Carman and Henry, 2007). To test whether expression of a curvature-stabilizing protein would convert the sheets into tubules, we used *opi1Δ* cells that express GFP-Rtn1p from the chromosome as well as the luminal ER marker ssRFP-HDEL. The overexpression of untagged Rtn1p from a CEN plasmid led to a partial conversion of sheets into tubules (Figure 6F; quantification in Figure 6H). When untagged Rtn1p was expressed at a still higher level from a 2μ plasmid, the sheet-to-tubule ratio converted back to about the level seen in wild type cells (Figure 6G and H). These data support the idea that the abundance of the reticulons determines the relative amounts of sheets and tubules in the cell.

A model for the generation of ER sheets and tubules

To test whether the curvature-stabilizing proteins alone could explain the relative amounts of sheets and tubules in a cell, we developed a simple theoretical model. We assume that the reticulons and DP1/Yop1p localize exclusively to tubules and sheet edges, generating and stabilizing these high curvature membranes by forming oligomeric scaffolds that are shaped as rigid arcs. Based on previous estimates, the energetically optimal distance between the arcs is assumed to be 40 nm (Hu et al., 2008). The edge membrane can be seen as a half-cylinder, whose axis bends in the sheet plane forming the sheet circumference. The protein driven formation of a sheet edge enables the two membranes of a sheet to adopt planar

shapes (Figure 7A). A tubule forms by self-folding of a part of the edge into a complete cylinder and therefore represents an edge extension (Figure 7A). We assume negligible bulging between the arc-like scaffolds, as supported by previous results (Hu et al., 2008), and a diameter of 30 nm for both sheet edges and tubules (Figure 4; (Bernales et al., 2006).

Our model calculates for a given membrane surface area the total length of the tubules and the shape and dimensions of the sheets in dependence of the number of curvature-stabilizing proteins, N_c. We characterize the edge length by a parameter $\Gamma = L_e/L_e^0$, where L_e^0 is the circumference of a flat circular disc with the same overall membrane area (i.e. Γ=1 for a flat disc). Γ is proportional to N_c (Supplemental Information). In our calculations we assume that N_c is at least large enough to generate a circular sheet ($\Gamma > 1$).

For each Γ value, we computed the overall membrane shape by minimizing the energy of the edge bending in the sheet plane (see Experimental Procedures and Supplemental Information). The top view of the shapes is presented in Figure 7B. Starting from the circular disc configuration at Γ=1 (Figure 7B, blue line), the sheet shape elongates with increasing Γ (and N_c) (light blue line), then acquires a flattened dumbbell appearance with a narrowing neck (aqua and yellow lines) and, finally, at Γ~2, splits into two droplet-like sheets with a short tubule between them (orange line). Further increase of Γ results in tubule elongation and a decrease in the sizes of the two sheets (Figure 7B, dark red line). Eventually, the whole membrane converts into a tubule (not shown in Figure 7B). Thus, the curvature-producing proteins alone can generate both sheets and tubules and their abundance determines the relative amounts of the two membrane domains.

Next, we extended the model to include the effect of proteins enriched in sheets. We assume that polysome-bound Climp63, p180, kinectin, as well as translocons can diffuse throughout the sheets, but cannot move into high curvature membrane areas, i.e. sheet edges and tubules. The number of all of these “sheet proteins” together is denoted by N_s. The sheet proteins may be considered as generating an “osmotic pressure” on the sheet edges, a force that resists the shrinkage of a sheet domain. The magnitude of this effect is determined by the interplay between the effective “osmotic pressure” produced by the sheet proteins and the effective stretching elasticity of the edge, the latter being determined by the curvature-stabilizing proteins (see Experimental Procedures and Supplemental Information). Our model does not take into account that Climp63 affects sheet formation by serving as a luminal spacer, and it does not make any assumptions about the specific roles of p180 and kinectin.

We computed the Γ values and membrane configurations for different values of N_c and N_s (Figure 7C). The colored lines on the bottom plane of the diagram represent the relationship between N_c and N_s for a given shape of the system, with the colors corresponding to the shapes as in Figure 7B. Figure 7C demonstrates that an increase of N_c at a given N_s results in larger Γ (blue to red transition) and thus in more tubules (Figure 7B), while an increase of N_s at a given N_c results in lower Γ, i.e. more sheets. This is further illustrated in Figure 7D, where the increase of N_s at a constant N_c converts two small sheet areas connected by a narrow tubule into a larger sheet area. Thus, the model recapitulates the experimental observation of a “tug-of-war” between sheet-promoting Climp63 and curvature-stabilizing proteins.

Discussion

Our results indicate that several mechanisms shape peripheral ER sheets. The most basic and universal mechanism appears to involve the previously identified curvature-stabilizing proteins, the reticulons and DP1/Yop1p. These proteins would not only stabilize the high

curvature of narrow tubules, but also the curvature of sheet edges, a mechanism that is sufficient to keep the two membranes of a sheet closely apposed. The reticulons and DP1/Yop1p probably stabilize high curvature by two mechanisms, “hydrophobic insertion/wedging” and “scaffolding” (Shibata et al., 2009). The conserved segments of these proteins may form a wedge in the lipid bilayer that occupies more space in the cytoplasmic leaflet than in the luminal leaflet. Oligomerization of these proteins may generate scaffolds around curved membranes, which may take the shape of open arcs, given that they can localize to sheet edges. Our theoretical model demonstrates that the reticulons and DP1/Yop1p alone can generate both tubules and sheets, with their abundance determining the ratio of these domains. Consistent with the proposed dual role of the reticulons and DP1/Yop1p in tubule and sheet formation, they localize to both tubules and sheet edges, their depletion leads to increased sheet areas, and their overexpression converts sheets into tubules.

In *S. cerevisiae* the amount of membrane surface and the abundance of the reticulons and Yop1p appear to be the decisive factors determining the ratio of peripheral ER sheets and tubules. Generating more lipid increases the sheet area, while increasing the abundance of the curvature-stabilizing proteins increases the amount of tubules. The observation of sheets in cells lacking the reticulons and Yop1p may be explained by the presence of other, low abundance curvature-promoting proteins, or by the association of the cortical ER with the plasma membrane. Although we cannot exclude the existence of sheet-promoting proteins in yeast, the current data are consistent with a model in which curvature-stabilizing proteins are the major determinant of peripheral ER morphology.

Our data suggest that in mammalian cells there are several additional factors that determine the morphology of peripheral ER sheets. This includes the coiled-coil membrane protein Climp63, which serves as a luminal spacer. After its depletion, the luminal width of the sheets decreases from ~50 to ~30 nm, a spacing that is also seen in organisms that lack the protein. Climp63 is highly upregulated in mammalian cells with proliferated ER sheets and it induces sheets at the expense of tubules when overexpressed in tissue culture cells. Thus, at high concentrations, Climp63 appears to generate sheets all by itself, and the lack of extensive sheet edges may make the contribution of the curvature-stabilizing proteins less important. However, with luminal spacers alone, one would expect bulging of the sheet edges, in contrast to our observations (Figure 4), indicating that the curvature-stabilizing proteins may have a role even in cells with proliferated ER sheets. Climp63’s function might be to optimize the size of the luminal space of peripheral ER sheets, such that sufficient luminal chaperones can be accommodated and the sheets are packed into a minimal space.

Our analysis also identified two other coiled-coil membrane proteins, p180 and kinectin, with a potential role in shaping ER sheets. These proteins are enriched in sheets and abundant in cells with proliferated ER sheets. Overexpression of p180 has been reported to induce sheets in *S. cerevisiae* and in a monocytic cell line (Becker et al., 1999; Benyamini et al., 2009), although in our own experiments and those of others the effects were smaller (Ueno et al.), 2010 and data not shown). The depletion of p180 and kinectin had no effect on ER sheet morphology. Although the precise role of these proteins remains to be established, all coiled-coil membrane proteins could stabilize sheets simply by being excluded from high-curvature regions, as shown by our theoretical considerations. They may be considered as generating an “osmotic pressure,” a force that counteracts the shrinkage of sheet domains. Consistent with experimental observations for Climp63, the coiled-coil proteins are predicted to be in a “tug-of-war” with the reticulons and DP1/Yop1p, with the former shifting the balance towards sheets and the latter towards tubules. In this model it does not actually matter how proteins are excluded from tubules and sheet edges. Given that all identified sheet-promoting proteins contain extended coiled-coil domains, they all have the

propensity to oligomerize, which may contribute to their exclusion from high-curvature regions.

The coiled-coil membrane proteins are not essential for sheet formation *per se*, as is obvious from our observation that their depletion by RNAi does not abolish ER sheets. This suggests that, like in yeast, the reticulons and DP1/Yop1p may provide the basic mechanism by which both sheets and tubules are generated. Consistent with this hypothesis, Climp63, p180, and kinectin are not known in lower organisms, in contrast to the reticulons and DP1/Yop1p, which are present in all eukaryotes.

All sheet-enriched proteins tested, including translocon components and the coiled-coil membrane proteins, appear to be concentrated by membrane-bound polysomes; upon polysome disassembly, all these proteins distribute equally between sheets and tubules throughout the cell. Thus, these proteins must have a direct or indirect affinity for membrane-bound polysomes. Indeed, several of the tested sheet-preferring proteins are known to be associated with membrane-bound translating ribosomes, including components of the Sec61 complex, the TRAP complex, the oligosaccharyl transferase complex, and p180 (Gorlich and Rapoport, 1993). These proteins stay bound to ribosomes upon detergent solubilization of rough ER membranes, but they can be released from the ribosomes by puromycin/high salt treatment. Climp63 and kinectin are not bound to detergent-solubilized translocons (data not shown), so how they are recruited remains to be clarified.

Our results indicate that ER sheets correspond to rough ER and tubules to smooth ER. We propose that the assembly of translating membrane-bound ribosomes into polysomes concentrates the associated membrane-proteins, including Climp63, p180, and kinectin. Their concentration might facilitate their higher-order oligomerization, which may be required for their exclusion from high-curvature areas and thus for their sheet-promoting function. Once sheets are formed, the membrane binding of polysomes would be facilitated. Polysomes often form spirals that could have an inherent preference for associating with ER sheets (Christensen and Bourne, 1999); while individual ribosomes or small polysomes can bind to narrow tubules, it is unlikely that each ribosome of a large polysome could be efficiently arranged on a narrow tubule. The binding of large polysomes could therefore be restricted to membrane sheets. The assembly of membrane-bound polysomes would concentrate more coiled-coil membrane proteins, and these in turn would generate more sheet area by the “osmotic effect,” allowing more polysomes to bind, and so on, a mechanism that would ultimately lead to a segregated rough ER domain. This model is consistent with the observation that the disassembly of polysomes or the depletion of Climp63 increases the mobility of translocons in the plane of the membrane (Nikonov et al., 2007; Nikonov et al., 2002). It also agrees with our results showing that the disassembly of polysomes leads to the spreading of ER sheets similar to that seen upon depletion of the sheet-promoting proteins. Our model explains the classic observation that in many cells membrane-bound ribosomes are not randomly distributed throughout the ER, but rather concentrated in a separate membrane domain, the rough ER. An active sorting of proteins into the rough ER is consistent with previous cell fractionation experiments, which demonstrated that general ER proteins indiscriminately distribute throughout the ER, whereas translocon-associated proteins are enriched in the rough ER (Hinman and Phillips, 1970; Kreibich et al., 1978; Vogel et al., 1990).

The nuclear envelope is a prominent ER domain whose structure is determined independently of the peripheral ER. Although the reticulons have been implicated in the assembly of the nuclear envelope and in the insertion of nuclear pores (Anderson and Hetzer, 2008; Dawson et al., 2009), they are nearly absent from the nuclear envelope, and their depletion or overexpression has no significant effect on this domain’s morphology.

Similarly, DP1/Yop1p or the coiled-coil membrane proteins Climp63, p180, and kinectin are also nearly absent from the nuclear envelope and have no obvious effect on its structure. Interestingly, TRAPα was also depleted from the nuclear envelope, raising the possibility that translocons are preferentially located in peripheral ER sheets. Thus, distinct mechanisms may determine the formation and function of the sheet-like domains of the nuclear envelope and peripheral ER.

In summary, our results lead to a simple model, according to which the basic morphological elements of the peripheral ER, the tubules and sheets, are generated by the curvature-stabilizing proteins. Superimposed on this mechanism, membrane-bound polysomes and associated coiled-coil membrane proteins may cooperate to form segregated rough ER sheets in mammalian cells, domains that are functionally specialized in protein translocation. Other factors probably contribute to the morphology of the peripheral ER. Microtubules keep the mammalian ER under tension and stabilize membrane tubules, but they could also potentially form an additional scaffold that stabilizes sheets, as suggested by the fact that both Climp63 and p180 are microtubule-binding proteins (Klopfenstein et al., 1998; Ogawa-Goto et al., 2007). It will be interesting to elucidate how these factors collaborate with the identified membrane-shaping principles.

Experimental Procedures

Mammalian tissue culture and transfections

COS7 and BSC1 cells stably expressing GFP-Sec61β were grown in DMEM containing 10% fetal bovine serum at 37°C and 5% CO_2, and passaged every 2–3 days. GFP-Dad1 BHK cells (M3/18; Nikonov et al, 2006) were maintained in 10% CO_2 at 39.5 °C to degrade endogenous Dad1. For translation inhibition experiments, cells were treated with 200 μM cycloheximide, 200 μM puromycin, or 100 nM pactamycin in complete media for 15 min.

To deplete Climp63, kinectin, and p180, COS7 cells were plated onto acid-washed coverslips at 20% confluency and transfected with 120 nM total siRNA using Oligofectamine (Invitrogen). 1.5 days later, cells were re-transfected with the same amount of siRNA oligonucleotides, and then processed for immunofluorescence 1.5 days afterwards. Experiments with control siRNA oligonucleotides (Qiagen) were done in parallel using the same conditions. Transient DNA transfections were performed using Lipofectamine 2000 (Invitrogen). See Supplemental Information for a list of DNA and siRNA constructs.

Indirect immunofluorescence and confocal microscopy

Indirect immunofluorescence with mammalian cells was done as described (Shibata et al., 2008). Cells grown on acid-washed coverslips were fixed with 4% paraformaldehyde (EMS), permeabilized with 0.1% TritonX-100 (Pierce), and immunostained with various primary antibodies, then washed in PBS and probed with various fluorophore-conjugated secondary antibodies. See Supplemental Information for a list of antibodies used.

Images were captured using a Yokogawa spinning-disk confocal on a Nikon TE2000U inverted microscope with a 60× or 100× Plan Apo NA 1.4 objective lens, a Hamamatsu ORCA ER-cooled CCD camera, and MetaMorph software. All analyses/quantifications were done on raw 16-bit images using MetaMorph. For presentation, brightness levels were adjusted across the entire image and were changed from 16- to 8-bits using Adobe Photoshop. Quantification was performed as described in Supplemental Information.

Thin section electron microscopy

Thin-section EM experiments were performed as described previously (Shibata et al., 2008), except that cells were fixed directly in culture plates. Quantification was performed as described in Supplemental Information.

Microscopy and image quantification of *S. cerevisiae* cells

Yeast strains and constructs used are described in Supplemental Information. Yeast cells were imaged live in complete medium at room temperature using an Olympus BX61 microscope, UPlanApo 100×/1.35 lens, Qimaging Retiga EX camera, and IVision version 4.0.5 software. To calculate relative peripheral sheet amounts, cortical ER images of cells expressing ssRFP-HDEL and Rtn1-GFP were taken. Images were thresholded above background, and the percentage of sheet area was calculated for each cell as the percentage of area of ssRFP-HDEL that did not overlap with Rtn1-GFP using Metamorph software. Means and standard errors were calculated using Microsoft Excel. For presentation, brightness levels were adjusted across the entire image, changed from 16- to 8-bits, and cropped using Adobe Photoshop.

Identification of abundant coiled-coil membrane proteins

Mass spectrometry of dog pancreatic microsomal proteins and identification of mRNAs coding for ER membrane proteins that are upregulated during B cell differentiation (Luckey et al., 2006) were performed as described in the Supplemental Information.

Modeling of sheet versus tubule generation

To compute the membrane configurations (the length of the tubule as well as the areas and shapes of the sheets) in dependence of the numbers of the curvature-producing, N_c, and the sheet-promoting proteins, N_s, we minimize the system energy, F_{tot}, for the given total membrane area, A_{tot}. The total energy F_{tot} consists of three contributions: the effective stretching energy of the edge, F_s; the energy of the effective "osmotic" pressure of the sheet-promoting proteins, F_p; and the energy of edge bending in the sheet plane, F_b.

The energy F_s is given by $F_s=\frac{1}{2}k_BTN_c\left[\frac{L_e-N_c(l_o+l_a)}{N_cl_o}\right]^2$, where, L_e is the total length of the edge including the tubules, l_o is the energetically preferred distance between the arc-like proteins measured along the edge; l_a is the width of one protein arc; $k_BT \approx 4 \cdot 10^{-21}$ Joule is the product of the Boltzmann constant and the absolute temperature. According to this expression, the length of the edge in a stress-free state is $L_e^*=N_c(l_0+l_a)$, and the effective rigidity of the edge stretching-compression with respect to L_e^* is $k_{str} = k_BT \cdot N_c$. Based on previous estimates, we take l_o = 40nm and l_a = 4nm (Hu et al., 2008).

The "osmotic pressure" energy F_p is given by $F_p=k_BT \cdot N_s \cdot \ln\left(\frac{N_sb}{A_{flat}}\right)$, where A_{flat} is the flat area available to the sheet proteins; b the area of one sheet protein. The area A_{flat} is related to the total length of the edge by $A_{flat}=\frac{1}{2}(A_{tot} - a \cdot L_e)$, where a is the membrane area absorbed by a unit length of the edge which can be estimated as $a = \pi \cdot R_e \approx$ 50nm ($R_e \approx$ 15nm is the radius of the edge cross-section) and A_{tot} is the total membrane area.

The energy F_b is given by $F_b=\frac{1}{2}B\oint c_e^2 dL_e$, where c_e is the in-plane curvature of the edge, and B is the modulus of the edge in-plane bending, which can be estimated using the membrane bending modulus $\kappa \approx 20k_BT$ (Helfrich, 1973) as $B \approx \pi R_e\kappa \approx 900\ k_BT \cdot$ nm. The integration is performed over the whole edge length including the tubules.

Estimates supported by numerical computations show that the total length of the edge L_e and the corresponding value of the parameter Γ are determined by the energies F_s and F_p and are largely independent of F_b. At the same time, the system configuration resulting from minimization of F_b depends of the parameter Γ. Therefore, we determine the system configuration in two steps.

First, we minimize the sum of $F_c + F_s$ with respect to L_e for every set of numbers N_c and N_s and determine the corresponding function $\Gamma(N_c, N_s)$. Second, for every value of $\Gamma(N_c, N_s)$, we minimize F_b with respect to the system shape and find the equilibrium configuration.

The Supplemental Information gives a more detailed discussion of the model.

Supplementary Material

Refer to Web version on PubMed Central for supplementary material.

Acknowledgments

We thank C. Denison, J. Minsteris and S. Gygi for mass spectrometry analysis; J. Baughman for microarray analysis; A. Condon for generating the ACY66 strain; A. Boye-Doe for cloning HA-Rtn4b; J. Iwasa for help with illustrations; G. Kreibich, K. Ogawa-Goto, L. Lu and R. Yan for materials; the Nikon Imaging Center and the electron microscopy facility at HMS for assistance; and R. Klemm and A. Osborne for critical reading of the manuscript. Y.S. is supported by the American Heart Association and W.A.P. by the Intramural Research Program of the National Institute of Diabetes and Digestive and Kidney Diseases. T.A.R is a Howard Hughes Medical Institute investigator.

References

Ambroziak J, Henry SA. INO2 and INO4 gene products, positive regulators of phospholipid biosynthesis in Saccharomyces cerevisiae, form a complex that binds to the INO1 promoter. J Biol Chem. 1994; 269:15344–15349. [PubMed: 8195172]

Anderson DJ, Hetzer MW. Reshaping of the endoplasmic reticulum limits the rate for nuclear envelope formation. J Cell Biol. 2008; 182:911–924. [PubMed: 18779370]

Baumann O, Walz B. Endoplasmic reticulum of animal cells and its organization into structural and functional domains. Int Rev Cytol. 2001; 205:149–214. [PubMed: 11336391]

Becker F, Block-Alper L, Nakamura G, Harada J, Wittrup KD, Meyer DI. Expression of the 180-kD ribosome receptor induces membrane proliferation and increased secretory activity in yeast. J Cell Biol. 1999; 146:273–284. [PubMed: 10427084]

Benyamini P, Webster P, Meyer DI. Knockdown of p180 eliminates the terminal differentiation of a secretory cell line. Mol Biol Cell. 2009; 20:732–744. [PubMed: 19037105]

Bernales S, McDonald KL, Walter P. Autophagy counterbalances endoplasmic reticulum expansion during the unfolded protein response. PLoS Biol. 2006; 4:e423. [PubMed: 17132049]

Carman GM, Henry SA. Phosphatidic acid plays a central role in the transcriptional regulation of glycerophospholipid synthesis in Saccharomyces cerevisiae. J Biol Chem. 2007; 282:37293–37297. [PubMed: 17981800]

Christensen AK, Bourne CM. Shape of large bound polysomes in cultured fibroblasts and thyroid epithelial cells. Anat Rec. 1999; 255:116–129. [PubMed: 10359513]

Dawson TR, Lazarus MD, Hetzer MW, Wente SR. ER membrane-bending proteins are necessary for de novo nuclear pore formation. J Cell Biol. 2009; 184:659–675. [PubMed: 19273614]

Gorlich D, Rapoport TA. Protein translocation into proteoliposomes reconstituted from purified components of the endoplasmic reticulum membrane. Cell. 1993; 75:615–630. [PubMed: 8242738]

Helfrich W. Elastic properties of lipid bilayers: theory and possible experiments. Z Naturforsch C. 1973; 28:693–703. [PubMed: 4273690]

Hinman ND, Phillips AH. Similarity and limited multiplicity of membrane proteins from rough and smooth endoplasmic reticulum. Science. 1970; 170:1222–1223. [PubMed: 5478197]

Hu J, Shibata Y, Voss C, Shemesh T, Li Z, Coughlin M, Kozlov MM, Rapoport TA, Prinz WA. Membrane proteins of the endoplasmic reticulum induce high-curvature tubules. Science. 2008; 319:1247–1250. [PubMed: 18309084]

Hu J, Shibata Y, Zhu PP, Voss C, Rismanchi N, Prinz WA, Rapoport TA, Blackstone C. A class of dynamin-like GTPases involved in the generation of the tubular ER network. Cell. 2009; 138:549–561. [PubMed: 19665976]

Klopfenstein DR, Kappeler F, Hauri HP. A novel direct interaction of endoplasmic reticulum with microtubules. Embo J. 1998; 17:6168–6177. [PubMed: 9799226]

Klopfenstein DR, Klumperman J, Lustig A, Kammerer RA, Oorschot V, Hauri HP. Subdomain-specific localization of CLIMP-63 (p63) in the endoplasmic reticulum is mediated by its luminal alpha-helical segment. J Cell Biol. 2001; 153:1287–1300. [PubMed: 11402071]

Kreibich G, Ulrich BL, Sabatini DD. Proteins of rough microsomal membranes related to ribosome binding. I. Identification of ribophorins I and II, membrane proteins characteristics of rough microsomes. J Cell Biol. 1978; 77:464–487. [PubMed: 649658]

Luckey CJ, Bhattacharya D, Goldrath AW, Weissman IL, Benoist C, Mathis D. Memory T and memory B cells share a transcriptional program of self-renewal with long-term hematopoietic stem cells. Proc Natl Acad Sci U S A. 2006; 103:3304–3309. [PubMed: 16492737]

Menetret JF, Hegde RS, Aguiar M, Gygi SP, Park E, Rapoport TA, Akey CW. Single copies of Sec61 and TRAP associate with a nontranslating mammalian ribosome. Structure. 2008; 16:1126–1137. [PubMed: 18611385]

Nikonov AV, Hauri HP, Lauring B, Kreibich G. Climp-63-mediated binding of microtubules to the ER affects the lateral mobility of translocon complexes. J Cell Sci. 2007; 120:2248–2258. [PubMed: 17567679]

Nikonov AV, Snapp E, Lippincott-Schwartz J, Kreibich G. Active translocon complexes labeled with GFP-Dad1 diffuse slowly as large polysome arrays in the endoplasmic reticulum. J Cell Biol. 2002; 158:497–506. [PubMed: 12163472]

Ogawa-Goto K, Tanaka K, Ueno T, Tanaka K, Kurata T, Sata T, Irie S. p180 is involved in the interaction between the endoplasmic reticulum and microtubules through a novel microtubule-binding and bundling domain. Mol Biol Cell. 2007; 18:3741–3751. [PubMed: 17634287]

Puhka M, Vihinen H, Joensuu M, Jokitalo E. Endoplasmic reticulum remains continuous and undergoes sheet-to-tubule transformation during cell division in mammalian cells. J Cell Biol. 2007; 179:895–909. [PubMed: 18056408]

Savitz AJ, Meyer DI. Identification of a ribosome receptor in the rough endoplasmic reticulum. Nature. 1990; 346:540–544. [PubMed: 2165568]

Schuck S, Prinz WA, Thorn KS, Voss C, Walter P. Membrane expansion alleviates endoplasmic reticulum stress independently of the unfolded protein response. J Cell Biol. 2009; 187:525–536. [PubMed: 19948500]

Senda T, Yoshinaga-Hirabayashi T. Intermembrane bridges within membrane organelles revealed by quick-freeze deep-etch electron microscopy. Anat Rec. 1998; 251:339–345. [PubMed: 9669761]

Shibata Y, Hu J, Kozlov MM, Rapoport TA. Mechanisms shaping the membranes of cellular organelles. Annu Rev Cell Dev Biol. 2009; 25:329–354. [PubMed: 19575675]

Shibata Y, Voeltz GK, Rapoport TA. Rough sheets and smooth tubules. Cell. 2006; 126:435–439. [PubMed: 16901774]

Shibata Y, Voss C, Rist JM, Hu J, Rapoport TA, Prinz WA, Voeltz GK. The reticulon and DP1/Yop1p proteins form immobile oligomers in the tubular endoplasmic reticulum. J Biol Chem. 2008; 283:18892–18904. [PubMed: 18442980]

Short B, Haas A, Barr FA. Golgins and GTPases, giving identity and structure to the Golgi apparatus. Biochim Biophys Acta. 2005; 1744:383–395. [PubMed: 15979508]

Snapp EL, Hegde RS, Francolini M, Lombardo F, Colombo S, Pedrazzini E, Borgese N, Lippincott-Schwartz J. Formation of stacked ER cisternae by low affinity protein interactions. J Cell Biol. 2003; 163:257–269. [PubMed: 14581454]

Sparkes I, Tolley N, Aller I, Svozil J, Osterrieder A, Botchway S, Mueller C, Frigerio L, Hawes C. Five Arabidopsis reticulon isoforms share endoplasmic reticulum location, topology, and membrane-shaping properties. Plant Cell. 2010; 22:1333–1343. [PubMed: 20424177]

Toyoshima I, Yu H, Steuer ER, Sheetz MP. Kinectin, a major kinesin-binding protein on ER. J Cell Biol. 1992; 118:1121–1131. [PubMed: 1512292]

Ueno T, Tanaka K, Kaneko K, Taga Y, Sata T, Irie S, Hattori S, Ogawa-Goto K. Enhancement of procollagen biosynthesis by p180 through augmented ribosome association on the endoplasmic reticulum in response to stimulated secretion. J Biol Chem.

Voeltz GK, Prinz WA, Shibata Y, Rist JM, Rapoport TA. A class of membrane proteins shaping the tubular endoplasmic reticulum. Cell. 2006; 124:573–586. [PubMed: 16469703]

Voeltz GK, Rolls MM, Rapoport TA. Structural organization of the endoplasmic reticulum. EMBO Rep. 2002; 3:944–950. [PubMed: 12370207]

Vogel F, Hartmann E, Gorlich D, Rapoport TA. Segregation of the signal sequence receptor protein in the rough endoplasmic reticulum membrane. Eur J Cell Biol. 1990; 53:197–202. [PubMed: 1964414]

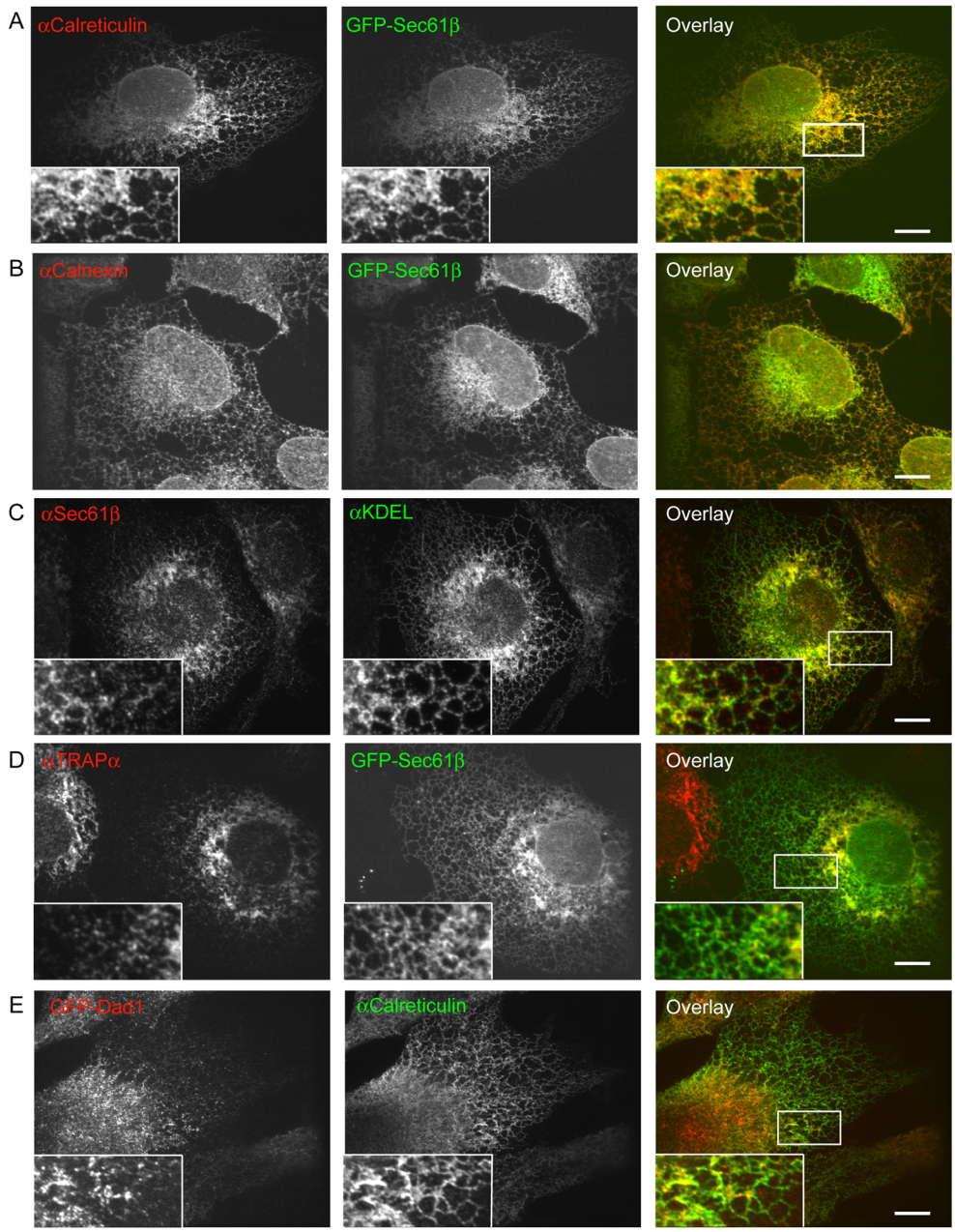

Figure 1. Localization of proteins to different ER domains

(A) The localization of endogenous luminal ER protein calreticulin is compared with that of the stably overexpressed membrane protein GFP-Sec61β using confocal microscopy in BSC1 cells. Calreticulin was detected with specific antibodies by indirect immunofluorescence (left panel) and Sec61β by GFP fluorescence (middle panel). The right panel shows a merged image. Junction between peripheral ER sheets and tubules are highlighted in the magnified view of the boxed area (inset). Scale bar, 10 μm.

(B) As in (A), but comparing the localization of the ER membrane protein calnexin with that of GFP-Sec61β.

(C) The localization of endogenous Sec61β is compared to that of the endogenous ER luminal proteins BiP and GRP94 (anti-KDEL), using indirect immunofluorescence with specific antibodies and confocal microscopy.

(D) As in (A), but comparing the localization of the translocon membrane protein TRAPα with that of GFP-Sec61β. Also note that TRAPα is noticeably depleted from the nuclear envelope.
(E) The localization of stably expressed GFP-Dad1 in a BHK cell line lacking endogenous Dad1 is compared with that of endogenous ER luminal proteins detected by calreticulin antibodies.
See also Figure S1.

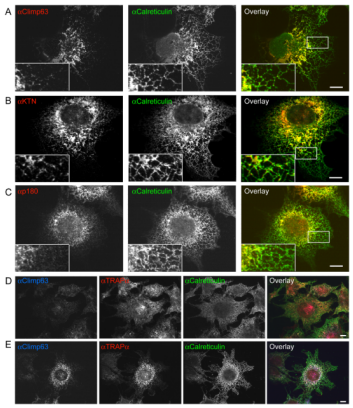

Figure 2. Membrane proteins enriched in ER sheets

(A) The endogenous localization of the membrane protein Climp63 is compared with that of the luminal ER protein calreticulin in COS7 cells, using indirect immunofluorescence with specific antibodies. The right most panel shows a merged image. Junction between peripheral ER sheets and tubules are highlighted in the magnified view of the boxed area (inset). Scale bar, 10 μm.

(B) As in (A), but comparing the localization of kinectin (KTN) and calreticulin.

(C) As in (A), but comparing the localization of p180 and calreticulin.

(D) Climp63, kinectin, and p180 were depleted in COS7 cells by RNAi, and Climp63, TRAPα, and calreticulin were visualized using indirect immunofluorescence with specific antibodies. Scale bar, 10 μm.

(E) As in (D), but with cells transfected with control siRNA oligonucleotides.

See also Figure S2 and S5.

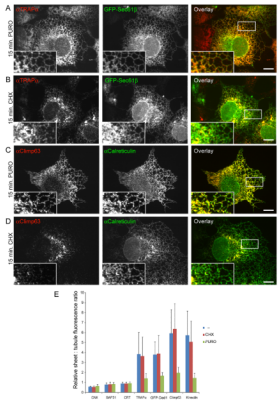

Figure 3. Polysome-dependent membrane protein enrichment in ER sheets

(A) The localization of the translocon component TRAPα is compared with that of stably expressed GFP-Sec61β after 15 min of treatment with puromycin (PURO). The right most panel shows a merged image. Junction between peripheral ER sheets and tubules are highlighted in the magnified view of the boxed area (inset). Scale bar, 10 μm.

(B) As in (A), but after 15 min of treatment with cycloheximide (CHX).

(C) As in (A), but comparing the localization of Climp63 with calreticulin after puromycin treatment.

(D) As in (C), but after cycloheximide treatment.

(E) Quantification of sheet enrichment of different ER proteins in untreated cells (blue bars) and in cells treated with puromycin (PURO; green) or cycloheximide (CHX; red). The ratio of the average fluorescence intensity in sheets versus tubules was determined for calnexin (CNX), BAP31, calreticulin (CRT), TRAPα, and kinectin, and divided by the sheet to tubule ratio for stably expressed GFP-Sec61β, a protein that shows no preference for either ER domain. A similar analysis was done for GFP-Dad1 and Climp63, but with calreticulin as reference. Shown are the means and standard errors of data obtained from 7 to 30 cells for each condition.

See also Figure S3 and S4.

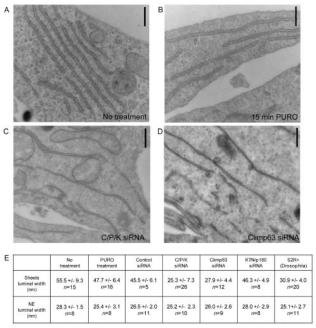

E

	No treatment	PURO treatment	Control siRNA	C/P/K siRNA	Climp63 siRNA	K1Nxy1b5 siRNA	S2R+ (Drosophila)
Sheets luminal width (nm)	55.6 +/- 9.3 n=10	47.7 +/- 6.4 n=10	45.5 +/- 6.1 n=5	25.3 +/- 7.3 n=26	27.9 +/- 4.4 n=12	46.3 +/- 4.9 n=8	30.9 +/- 4.0 n=20
NE luminal width (nm)	28.3 +/- 1.5 n=8	28.4 +/- 3.1 n=8	26.5 +/- 2.0 n=11	25.2 +/- 2.3 n=10	26.0 +/- 2.6 n=9	28.0 +/- 2.9 n=8	25.1 +/- 2.7 n=11

Figure 4. Climp63 affects the luminal width of peripheral ER sheets

(A) Rough ER sheets in a COS7 cell visualized by thin-section electron microscopy. Scale bar, 0.5 μm.

(B) As in (A), but after treatment with puromycin (PURO) for 15 min.

(C) As in (A), but after RNAi-depletion of Climp63, p180, and kinectin (C/P/K siRNA).

(D) As in (A), but after RNAi-depletion of Climp63.

(E) Quantification of the luminal width of peripheral ER sheets and the nuclear envelope (NE) in differently treated COS7 cells. For comparison, Drosophila S2R+ cells were also analyzed. Shown are the mean and standard error of *n* cells analyzed.

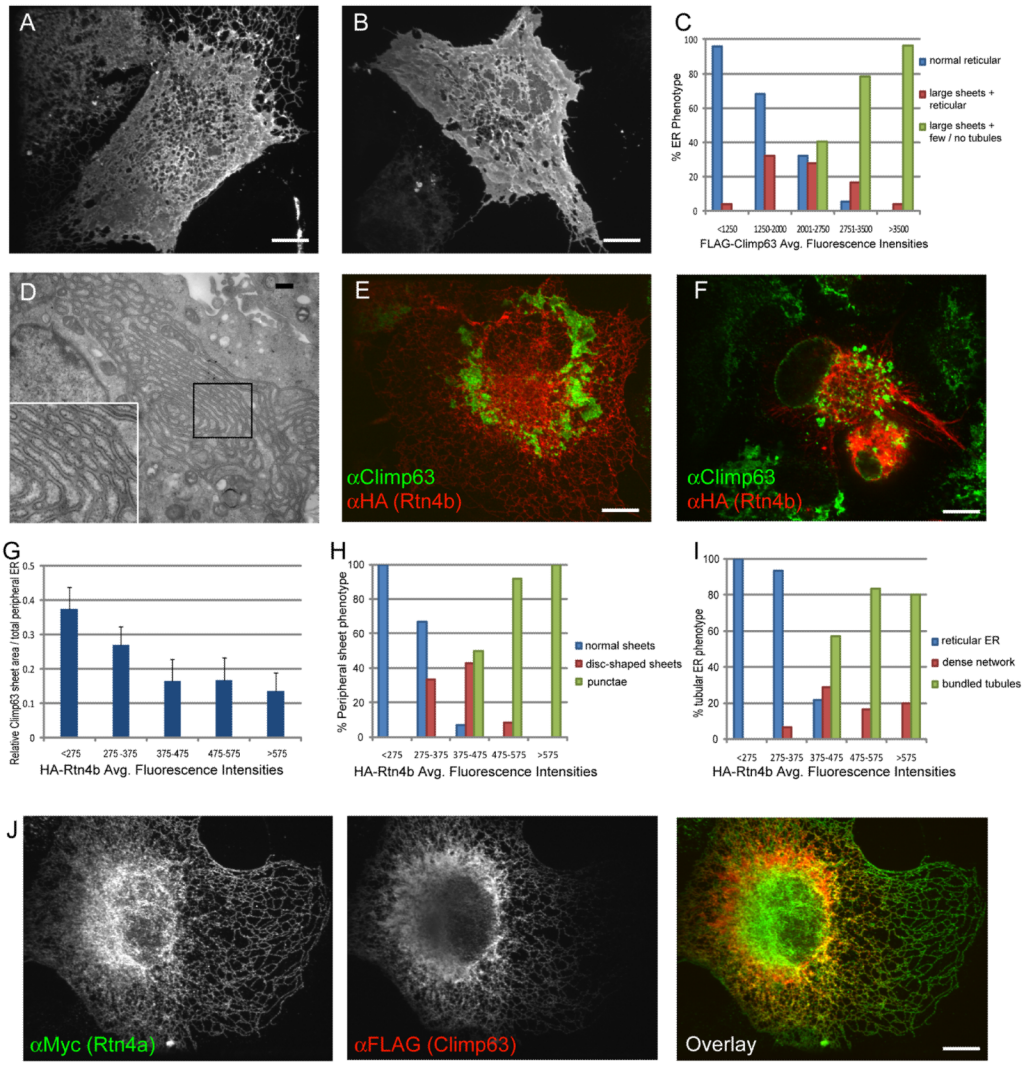

Figure 5. Climp63 and reticulon overexpression change the abundance of sheets and tubules

(A) FLAG-Climp63 overexpressed at relatively high levels in a COS7 cell was visualized by indirect immunofluorescence using FLAG antibodies. A 3D image was generated from a complete series of z-sections (step size 0.25 um) taken with a confocal microscope.

(B) As in (A), but in a cell expressing FLAG-Climp63 at the highest observed levels.

(C) Quantification of the effect of Climp63 overexpression on ER sheet abundance. Shown are the percentages of cells with normal reticular ER (blue bars), of cells with both large sheets and reticular ER (red), and of cells with large ER sheets lacking reticular ER (green) at different expression levels of FLAG-Climp63. The cells were divided into five groups according to their expression levels, determined by overall average fluorescence intensity.

(D) Thin-section electron micrograph of a COS7 cell overexpressing GFP-Climp63. The inset shows an enlargement of the boxed region. Scale bar, 0.5 μm.

(E) HA-Rtn4b (red) was expressed in COS7 cells at relatively low levels and localized with HA-antibodies by indirect immunofluorescence and confocal microscopy. Endogenous Climp63 (green) was localized in the same cells with specific antibodies.

(F) As in (G), but with the highest observed expression level of HA-Rtn4b. Note that Climp63 appears in bright punctae and in the nuclear envelope.

(G) Quantification of the peripheral ER sheet area relative to the total ER area for different expression levels of HA-Rtn4b. The areas of ER sheets and tubules were determined from the fluorescence of Climp63 and Rtn4b, respectively, after subtraction of background. The cells were divided into five groups according to their expression levels of HA-Rtn4b, determined by overall average fluorescence intensity, and the mean and stardard error were calculated.
(H) Quantification of the effect of Rtn4b overexpression on ER sheet morphology, as determined by Climp63 staining. Shown are the percentages of cells with normal ER sheets (blue bars), of cells with disc-like ER sheets (red), and of cells with punctae (green) at different expression levels of Rtn4b. The cells were divided into five groups according to their expression levels.
(I) Quantification of the effect of Rtn4b overexpression on ER tubule morphology, as determined by HA-Rtn4b staining. Shown are the percentages of cells with normal reticular ER (blue bars), of cells with an abnormally dense ER network (red), and of cells with unbranched, long tubules (green) at different expression levels of Rtn4b. The cells were divided into five groups according to their expression levels.
(J) Myc-Rtn4a and FLAG-Climp63 were both highly expressed in COS7 cells. The right most panel shows a merged image. Note that the ER morphology is almost normal.
See also Figure S6 and S7.

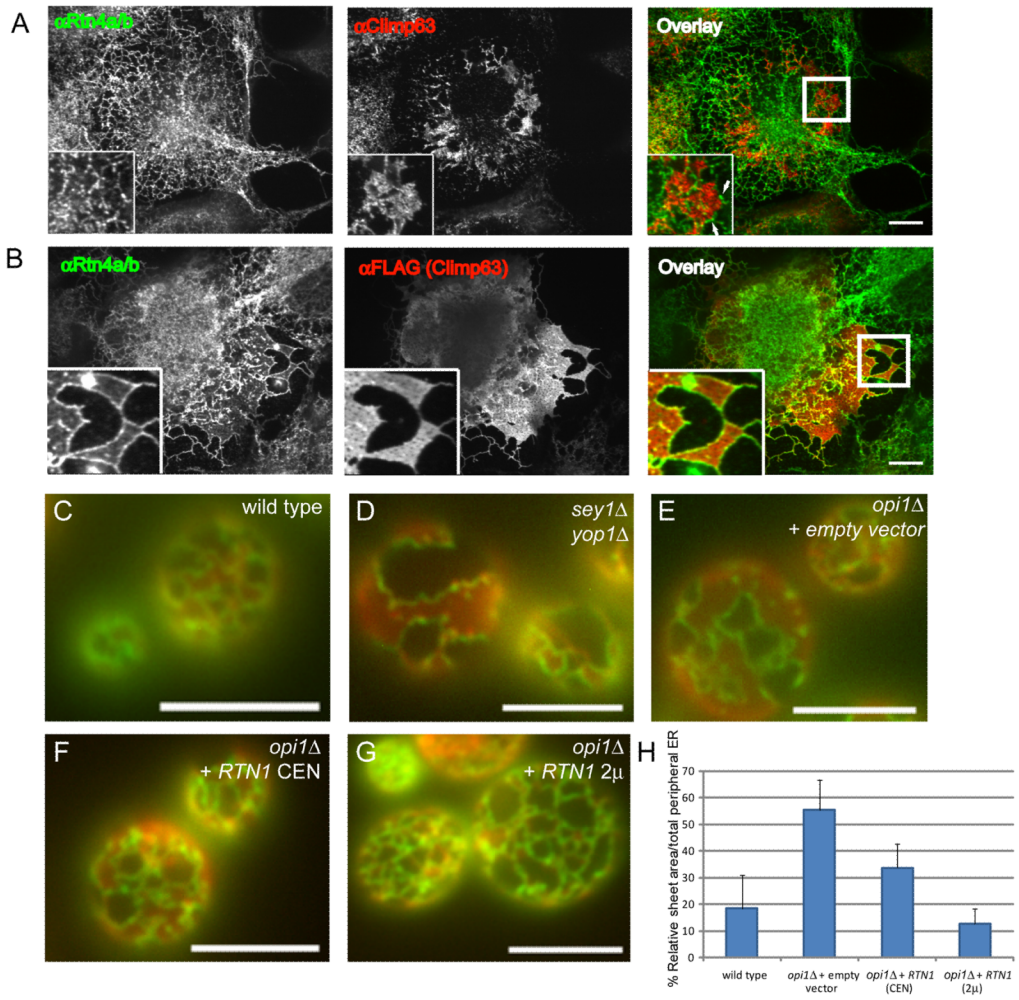

Figure 6. The reticulons localize to the edges of ER sheets

(A) The localization of endogenous Rtn4a and 4b is compared with that of Climp63 using indirect immunofluorescence with specific antibodies in COS7 cells. The lower row panels show enlargements of the boxed region. Arrows point to reticulons lining the sheets. The right most panel shows merged images.

(B) As in (A), but with cells overexpressing FLAG-Climp63.

(C) GFP-Rtn1p (green) and ssRFP-HDEL (red) were co-expressed in wild type *S. cerevisiae* cells and the cortical ER was visualized by fluorescence microscopy. Scale bar, 5 μm.

(D) As in (C), except that the cells had proliferated ER sheets caused by deletion of *SEY1* and *YOP1 (sey1Δyop1Δ).*

(E) As in (C), except the cells had proliferated ER sheets caused by deletion of *OPI1 (opi1Δ).* The cells also contained an empty vector as a control for panels (F) and (G).

(F) As in (E), except that untagged Rtn1p was expressed under the endogenous promoter from a CEN plasmid.

(G) As in (E), except that untagged Rtn1p was expressed under the endogenous promoter from a 2μ plasmid.

(H) Quantification of the experiments in (C) and (E–G). The relative area of ER sheets was determined from the area of ssRFP-HDEL fluorescence that did not co-localize with GFP-Rtn1p fluorescence and divided by the total area of ssRFP-HDEL fluorescence. 14 to 38 cells were analyzed and the mean and standard error were calculated.

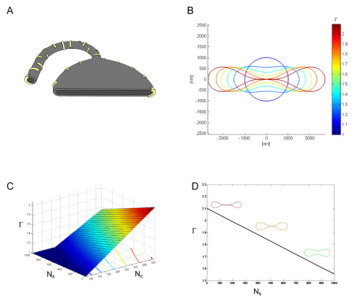

Figure 7. Modeling of the effect of curvature-stabilizing and sheet-promoting proteins on ER morphology

(A) The reticulons and DP1/Yop1p (yellow arcs) are assumed to localize exclusively to tubules and sheet edges, generating and stabilizing these high curvature membranes. Stabilization of sheet edges enables the upper and lower membranes of the sheet to adopt planar shapes.

(B) Top view of membrane shapes computed by the theoretical model for increasing Γ values. The computation was performed for a total membrane area corresponding to 1μm radius of the initial disc-like shape, a 15nm cross-section radius of the tubules and edges, and a 40 nm optimal distance between the arc-like proteins at the edge (see Supplemental Information). Change of Γ from 1 to 2.1(blue to red) corresponds to increasing the number of curvature-stabilizing proteins N_c from 140 to 290.

(C) Γ values and membrane shapes were calculated for different numbers of curvature-stabilizing and sheet-promoting proteins, N_c and N_s. The colors correspond to the membrane shapes shown in Figure 7B. The colored lines on the bottom plane of the diagram represent the relationship between N_c and N_s for a given shape of the system.

(D) Γ values and membrane shapes were computed for different N_s values at N_c = 290. The shapes refer to N_s = 0, 500, and 1000.